V

Scotti, G., Kanninen, P., Mäkinen, M., Kallio, T., Franssila, S.: Silicon nanograss as micro fuel cell gas diffusion layer, *Micro & Nano Lett.* **5** (2010) 382-385.

Silicon nanograss as micro fuel cell gas diffusion layer

G. Scotti[1,3], P. Kanninen[2], M. Mäkinen[3], T. Kallio[2], S. Franssila[3]

[1]*Department of Micro and Nanosciences, Aalto University School of Science and Technology, P.O. Box 13500, Aalto 00076, Espoo, Finland*
[2]*Department of Chemistry, Aalto University School of Science and Technology, P.O. Box 16100, Aalto 00076, Espoo, Finland*
[3]*Department of Materials Science and Engineering, Aalto University School of Science and Technology, P.O. Box 16200, Aalto 00076, Espoo, Finland*
E-mail: gianmario.scotti@tkk.fi

Published in Micro & Nano Letters; Received on 16th August 2010; Revised on 26th October 2010

This Letter describes a microfabricated fuel cell (MFC) that uses hydrogen as fuel and a polymer proton exchange membrane as electrolyte. Microchannels have been etched in highly conductive silicon, and silicon nanograss (black silicon) has been formed on the surface; thus implementing a support structure, current collector, flowfield and gas diffusion layer all in one. The devices are thus very compact, simple to fabricate and low cost. The MFC presented here shows promising performance of 70 mW cm^{-2} power density and 100 mA cm^{-2} current density at 0.7 V, comparable to that of other similar monolithic devices found in the literature.

1. Introduction: In recent years, there has been a growing interest in replacing conventional lithium ion batteries with fuel cells as power sources for portable electronic devices (laptops, handheld cameras, mobile phones etc.) to achieve higher energy densities [1]. Microfabrication technologies enable highly integrated, compact micro fuel cells. The most promising fuel candidates are hydrogen and methanol. Many of the micro fuel cells are made from silicon because it is the material for which there is most microfabrication expertise: thin film processes (evaporation, sputtering, chemical vapour deposition, oxidation etc.) and dry and wet etching chemistries are implemented and well optimised for silicon as a substrate. Furthermore, silicon is hard, durable and has reasonable chemical and thermal stability. The electrochemical properties of silicon are extensively researched and documented.

In this work, the authors show how silicon microfabrication technologies enable them to integrate flow channels, electrodes, gas diffusion layer (GDL) and current collection into a single structure, with a very small number of fabrication steps. Owing to the integration of the GDL with the current collector and flowfield, and the lack of many metallisation or other layers (mechanical support, current collector, insulation, gas distribution, electrical distribution etc.), the device is very compact (very thin) which can lead to high volumetric power densities. Other authors [2–6] have also integrated macroporous silicon (IUPAC term for pores larger than 50 nm) GDL, the flowfield and the current collector into a monolithic silicon unit using microfabrication techniques. This device, however, shows that integration can be carried much further, while simultaneously simplifying the fabrication process. The term 'flowfield body' is used to denote the structure consisting of the current collector, the flowfield and the GDL. This distinguishes it from electrodes, which in this case are part of the membrane-electrode assembly (MEA) and consist of carbon black with platinum nanoparticles, spray-painted onto the polymer electrolyte membrane (PEM).

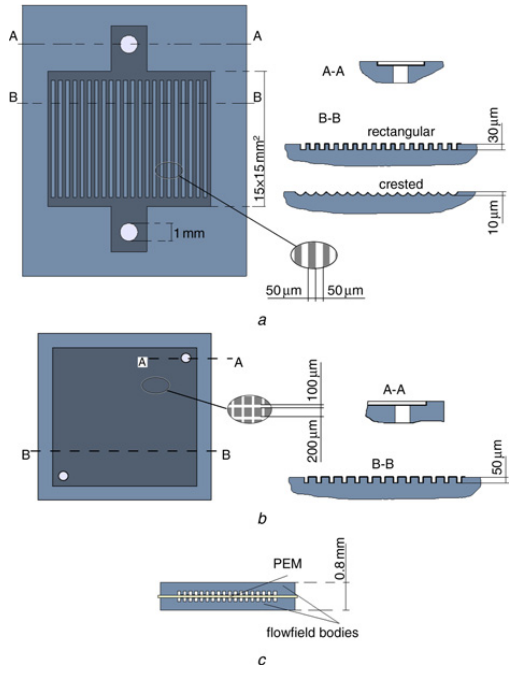

Figure 1 *Construction of a single flowfield body (top views and cross-sections)*
a For the symmetric
b Diagonal flow design
c Assembly of a fuel cell

2. Experimental

2.1. Construction: The authors have designed and fabricated three devices with the main difference between them being the profile (crested and rectangular) and topology (straight and serpentine grooves, and pillars) of the flowfield channels. Fig. 1 depicts the construction of the flowfield bodies (*a* and *b*), and the assembly of a fuel cell (*c*), composed of two flowfield bodies with a PEM (Nafion®) sandwiched between them. The gas inlet holes introduce the reactant gases into the flowfield and the GDL.

2.2. Fabrication: A detailed description of the fabrication of a fuel cell with rectangular flowfield channels will be presented. The main difference in fabrication in the case of the crested profile channels is an isotropic reactive ion etching (RIE) step. More information on the crested profile flowfield fabrication can be found in [7].

The starting point for the flowfield body is a highly boron-doped ($\rho = 0.01\ \Omega$ cm), thermally oxidised silicon wafer. The main fabrication steps for the flowfield bodies are presented in Fig. 2: the

doi: 10.1049/mnl.2010.0122

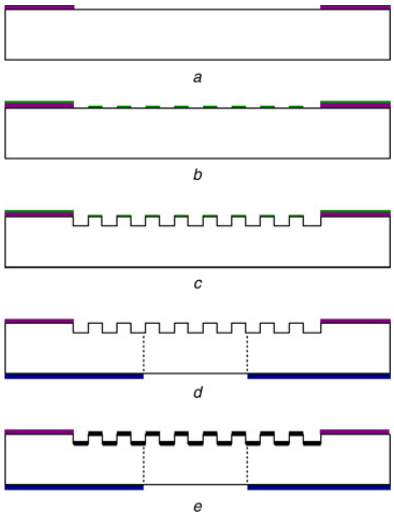

Figure 2 *Process flow for the fabrication of square profile flowfield body with gas inlets, flowfield and gas diffusion layer*
a Pattern SiO_2 to define the black silicon area
b Pattern the mask for the flowfield
c RIE of flowfield, 30–50 μm deep
d Backside gas inlet etch through AI mask
e Black silicon formation and metalisation
Details are provided in the text

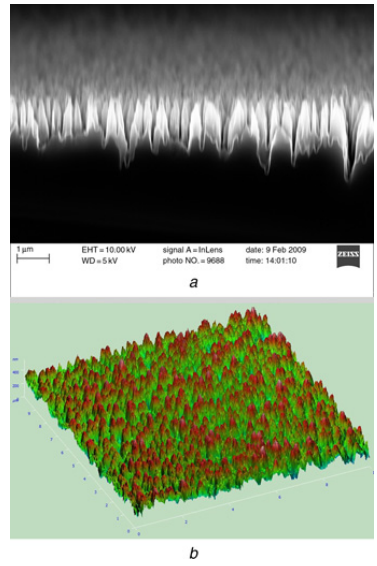

Figure 3 *Characterisation of silicon nanograss*
a SEM
b AFM micrographs

thermally oxidised wafer (oxide thickness of about 300 nm) is patterned with photolithography and buffered hydrofluoric acid etching (Fig. 2*a*) to delimit the area affected by silicon nanograss formation later on. Thin resist (AZ 1505®, 0.5 μm thick with spinning at 4000 RPM) is spun and patterned, to function as an etch mask (Fig. 2*b*), followed by a silicon deep RIE (DRIE) etch step performed in a cryogenic inductively coupled plasma (ICP) RIE (Oxford Instruments Plasmalab® System 100) in SF_6/O_2 (etch parameters: ICP 2 kW, CCP 3 W, SF_6 flow 100 sccm, O_2 flow 15 sccm, pressure 10 mTorr, temperature −110°C) (Fig. 2*c*). Processing under these conditions results in ∼30 μm deep channels after 5 min of etching and 50 μm tall square pillars after 7.5 min. On the backside of the wafer a 200 nm aluminium layer is deposited by sputtering (Plasmalab® System 400) and patterned with commercial H_3PO_4-based wet etchant. This layer acts as an etch mask for through-wafer DRIE etching for the gas inlets (Fig. 2*d*). The inlet etching process is identical to flowfield etching process. Finally, nanograss (black silicon) is formed by plasma etching under passivating conditions (ICP 1 kW, CCP 2W, SF_6 flow 40 sccm, O_2 flow 18 sccm, $p = 10$ mTorr, $T = -120$°C, $t = 10$ min) (Fig. 2*e*) on the area (on the top side) unprotected by thermal oxide.

Scanning electron microscopy (SEM) and atomic force microscopy (AFM) micrographs of the resulting silicon nanograss are shown in Fig. 3. As the last microfabrication step, a thin metallisation layer (30 nm of chromium or 30 nm platinum) is sputtered over the nanograss to improve electrical conductivity. Fig. 4 shows SEM micrographs of the three microfabricated fuel cell (MFC) flowfields.

Table 1 summarises the differences between the three flowfields studied in this Letter. It should be noted that the isotropic etching of the crested channels can leave residues of masking material in the ICP RIE chamber as it tends to snap away from the silicon. In the square profile flowfield fabrication this would not happen, as anisotropic etching does not create undercut. For the flowfield etch, a thin photoresist (AZ® 1505) mask suffices for short etch times of about 5 min. The authors chose a thin photoresist because at −110°C thicker photoresist layers would crack [8]. However, on the backside an aluminium mask is necessary because the through-wafer etch lasts much longer, whereas a photoresist layer would not survive. This aluminium layer serves also as current collector and electrical contact. While the through-wafer etch process parameters are identical to the ones for the flowfield etching, the etch rate is higher; about 7 μm min^{-1} against 5 μm min^{-1}, because the etched area is smaller (smaller etch loading).

The MEA is Nafion® 115 coated with catalyst using a modification of the thin-film method developed by Wilson and Gottesfeld [9]: carbon supported catalyst (60% platinum, 40% carbon, from Alfa Aesar) is mixed with a 5 wt% Nafion® solution (Aldrich) by magnetic stirring and sonication to produce a catalyst ink. The viscosity of the solution is controlled by adding methanol. This ink is sprayed on the membrane by an air brush through a stencil, to form a uniform, thin catalyst layer on the membrane. After both sides of the membrane have been painted with adequate amount of catalyst material, the membrane is hot-pressed (140°C, 50 kN, 2 min). The finalised catalyst layer contains approximately 40 wt% of platinum, 30 wt% of carbon support and 30 wt% of Nafion® polymer. The loading of platinum is approximately 0.5 mg cm^{-2} per side.

2.3. Measurements: The micro fuel cells were characterised by clamping them in a custom-built fixture made from two aluminium blocks fitted with threaded gas holes and sockets for electrical contacts. Each block has dimensions 44 × 62 mm and is 10 mm thick. A photograph of the fixture connected to gas sources and electric measurement equipment is presented in Fig. 5. The reactant gases were pure, humidified oxygen and hydrogen, flowing at 50 ml min^{-1} and at a temperature of ∼22°C. The load on the (electric) output of the MFC is swept with an Autolab® PGSTAT100 potentiostat from the maximum (open-circuit voltage) to 0.1 V, at a rate of 1 mV s^{-1}.

3. Results and discussion: All three cell designs were successfully fabricated. The measured current and power output results are summed up in Fig. 6. It is clear from the plots that the square-profile channel fuel cells are the best performance-wise. This performance is comparable to other hydrogen-fuel silicon MFCs

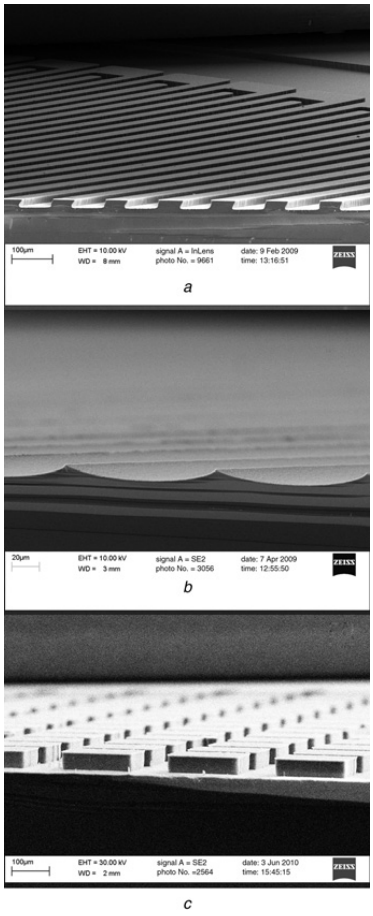

Figure 4 *SEM micrographs*
a Square profile
b Crested profile
c Rectangular pillar flowfield. Note the serpentine topology of the channels in *a*

recorded in the literature [2, 3, 6, 10, 11]. This design differs from previous MFCs in using a simple maskless process for forming an integrated silicon nanograss as GDL.

Both straight flow channels and serpentined flow channels with two bends triplicating the flow length (Fig. 4*a*) have been fabricated and characterised, but no difference in performance was measurable. It can be concluded that enough reactant gas diffuses through the GDL to neutralise any effects of a double-bend serpentine against a straight channel flowfield.

The metallisation on the silicon nanograss GDL, whether platinum or chromium, had no significant effect on the performance of the fuel cells. This is a significant finding as it eliminates one noble metal deposition. The performance difference that the various flowfields exhibit can be explained by different cross-sections of the channels and by different contact area between the MEA and the flowfield body. The square pillar flowfield channels have a larger cross-section ($50 \times 100\ \mu m^2$) compared to the straight square channels ($30 \times 50\ \mu m^2$). This could mean that because of the tighter flow geometry in square channels, reactant gases are pushed more efficiently into the black silicon area, thus improving the performance of these cells. Also, the pillars are wider (200 μm) than the ridges between square channels (50 μm), which means a longer gas permeation length in black silicon. In the case of crested profile, the cross-section is even smaller (less than $10 \times 100\ \mu m^2$) but in addition only a small area of the flowfield body is in contact with the MEA. Thus, a fewer number of black silicon needles in electrical contact with the MEA could explain the lower performance.

These rectangular profile fuel cells exhibit an abrupt and permanent degradation at a certain voltage (see the fold-back of the graphs for the square channel MFC on Fig. 6). This was not owing to water condensation since after drying the cell, the current density remained under 10 mA cm^{-2} at all potentials. Post-mortem analysis of the flowfield bodies and MEA (with SEM, AFM and Raman

Table 1 Summary of flowfield geometries

Flowfield type	Crested profile	Rectangular profile	Rectangular pillars
Channel depth, μm	10	30	50
Channel width, μm	100	50	100
Flowfield etch step	isotropic	anisotropic	anisotropic

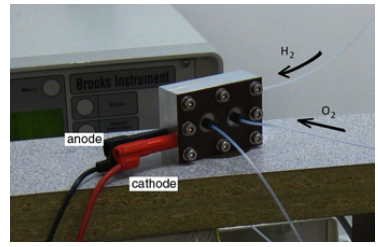

Figure 5 *Picture of the measurement setup with the jig clamping a measured MFC*

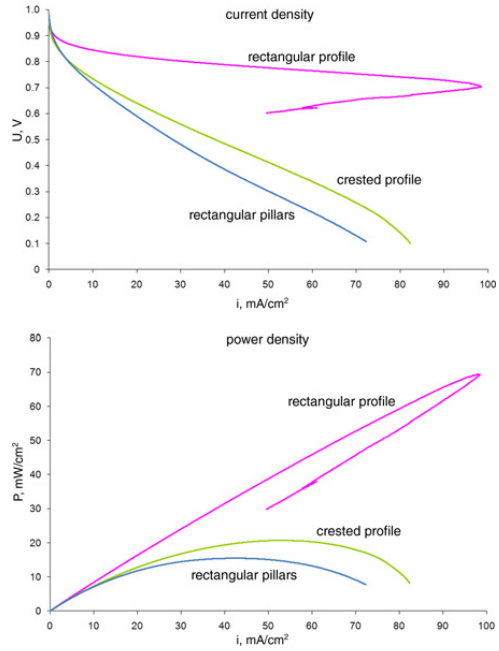

Figure 6 *Measured current and power density plots for all three types of micro fuel cells*

doi: 10.1049/mnl.2010.0122

Table 2 Comparison of maximum performances

Max. current and power densities	This work			Lee *et al.* [2]	Xiao *et al.* [3]	Kuriyama *et al.* [10]
	Crested	Rectangular	Pillars			
Current, mA cm^{-2}	82.3	98.5	73	38	72	260
Power, mW cm^{-2}	20.7	69.2	15.4	8.13	13.7	75

spectroscopy) was inconclusive. The behaviour is reproducible, but since the performance is high (much higher current densities could be reached if the degradation did not happen), further research will be completed to understand this problem. The devices with crested channel and square pillars did not exhibit this degradation.

This study confirms the feasibility of simple monolithic silicon MFCs where the GDL is created by etching a single-crystal silicon wafer, such as in [2–6], and improves their designs with the use of silicon nanograss and by a truly maskless fabrication (in contrast to previous silicon micropillars reported by Feng *et al.* [4]). The quasi-conical shape of the nanograss allows for easy metallisation via sputtering or evaporation. Most of the other authors have used a separate GDL, typically carbon fibre or carbon paper as part of a commercial MEA, even though other materials have been proposed, such as sintered steel mesh [12], dendritic platinum deposited by electroplating [11] and chemical vapour deposited carbon nanotubes [10]. Separate GDLs in MFCs are used because they are commercially available or because higher performance is achieved with them (Table 2).

This integrated design ensures good uniformity of electromechanical contact across the assembled device. This improves on the need for external fixtures [10]. The MFCs presented here do not require a noble metal layer for current collection, because the highly doped, thin silicon substrate itself acts as a current collector. Thick layers of gold [10, 11] or platinum [6] are commonly used for this purpose, especially in high-performance MFCs. For instance, Kuriyama *et al.* [10] evaporated 3 μm of gold to act as a current collector. Since the silicon nanograss GDL was fabricated from the same highly doped silicon bulk as the flowfield and current collector, the conductivity through the GDL is good. While the device in [10] does achieve slightly higher power density than that of the present device (75 against 70 mW cm^{-2}), their design requires considerably more materials and levels: glass interconnect structure with metallisation, silicon support structure, Au/Ti current collector, copper via metallisation with silver paste, MoSi and iron on SiO_2 for carbon nanotube (CNT) growth, the CNT GDL itself and so on. In contrast, the simple structure of the membrane-flowfield assembly allows for higher compactness and therefore overall thinner cells (0.8 mm) and higher volumetric power density. With fewer process steps, the likelihood for defects decreases and the authors have been able to fabricate fairly large area cells (2.25 cm^2) with high yield.

4. Conclusions: A simple, low-cost fabrication method has been presented for highly integrated micro fuel cells. The fabricated cells show performance comparable to the best hydrogen MFCs found in the literature. The elimination of a separate GDL and current collector has been achieved with silicon nanograss and highly boron-doped silicon main body, respectively. The simplicity of the design allows for easy miniaturisation and integration with other MEMS components. The small vertical dimensions make these fuel cells well suited for stacks in portable devices. The elimination of noble metals for current collection and GDL protection should bring sizable cost savings and open up possibilities for micro fuel cells to penetrate power source markets for portable devices.

5. Acknowledgments: The authors acknowledge Prof. Valentinas Snitka and Dr. Denys Naumenko, RC for Microsystems and Nanotechnology, Kaunas University of Technology for the AFM imaging, and the MIDE organization of the Aalto University School of Science and Engineering for the funding.

6 References

[1] Dyer C.K.: 'Fuel cells for portable applications', *Fuel Cells Bull.*, 2002, **2002**, (3), pp. 8–9

[2] Lee C.Y., Lee S.J., Hu Y.C., Shih W.P., Fan W.Y., Chuang C.W.: 'Integration of silicon micro-hole arrays as a gas diffusion layer in a micro-fuel cell', *Int. J. Hydrogen Energy*, 2009, **34**, pp. 6457–6464

[3] Xiao Z., Yan G., Feng C., Chan P.C.H., Hsing I.M.: 'A silicon-based fuel cell micro power system using a microfabrication technique', *J. Micromech. Microeng.*, 2006, **16**, pp. 2014–2020

[4] Feng C., Xiao Z., Chan P.C.H., Hsing I.M.: 'Lithography-free silicon micro-pillars as catalyst supports for microfabricated fuel cell applications', *Electrochem. Commun.*, 2006, **8**, pp. 1235–1238

[5] Aravamudhan S., Rahman A.R.A., Bhansali S.: 'Porous silicon based orientation independent, self-priming micro direct ethanol fuel cell', *Sens. Actuators A*, 2005, **123–124**, pp. 497–504

[6] Min K.B., Tanaka S., Esashi M.: 'Fabrication of novel MEMS-based polymer electrolyte fuel cell architectures with catalytic electrodes supported on porous SiO_2', *J. Micromech. Microeng.*, 2006, **16**, pp. 505–511

[7] Scotti G., Kanninen P., Kallio T., Franssila S.: Symmetric fuel cell with porous electrodes, technical digest transducers 2009 (Denver, Colorado, USA, 21–25 June 2009), pp. 1401–1404

[8] Sainiemi L., Franssila S.: 'Mask material effects in cryogenic DRIE', *J. Vac. Sci. Technol.*, 2007, **B25**, pp. 801–807

[9] Wilson M.S., Gottesfeld S.: 'High performance catalyzed membranes of ultra-low pt loadings for polymer electrolyte fuel cells', *J. Electrochem. Soc.*, 1992, **139**, pp. L28–L30

[10] Kuriyama N., Kubota T., Okamura D., Suzuki T., Sasahara J.: 'Design and fabrication of MEMS-based monolithic fuel cells', *Sens. Actuators A*, 2008, **145–146**, pp. 354–362

[11] Yeom J., Mozsgai G.Z., Flachsbart B.R., *ETAL.*: 'Microfabrication and characterization of a silicon-based millimeter scale, PEM fuel cell operating with hydrogen, methanol, or formic acid', *Sens. Actuators B*, 2005, **107**, pp. 882–891

[12] Liu J., Sun G., Zhao F., *ETAL.*: 'Study of sintered stainless steel fiber felt as gas diffusion backing in air-breathing DMFC', *J. Power Sources*, 2004, **133**, pp. 175–180